

# Learning to Approximate Computing at Run-time

Paulo Garcia, Mehryar Emambakhsh, Andrew Wallace

**Abstract**—Intelligent sensor/signal processing systems are increasingly constrained by tight power budgets, especially when deployed in mobile/remote environments. Approximate computing is the process of adaptively compromising over the accuracy of a systems output in order to obtain higher performance for other metrics, such as power consumption or memory usage, for applications resilient to inaccurate computations. It is, however, usually statically implemented, based on heuristics and testing loops, which prevents switching between different approximations at run-time. This limits approximation versatility and results in under- or over-approximated systems for the specific input data, causing excessive power usage and insufficient accuracy, respectively. To avoid these issues, this paper proposes a new approximate computing approach by introducing a supervisor block embedding prior knowledge about runtime data. The target system (i.e., signal processing pipeline) is implemented with configurable levels and types of approximations [1]. Data processed by the target system is analysed by the supervisor and the approximation is updated dynamically, by using prior knowledge to establish a confidence measure on the accuracy of the computed results. Moreover, by iteratively evaluating the output, the supervisor block can learn and subsequently update tunable parameters, in order to improve the quality of the results. Our approach also envisions switching between multiple approximation and learning engines at run-time. We detail and evaluate this approach for tracking problem in computer vision. Results show our approach yields promising trade-offs between accuracy and power consumption.

**Index Terms**—field programmable gate array (FPGA), optimizations, power, image processing, dataflow

## I. INTRODUCTION

Power/performance trade offs are well established compromises in the design of all embedded systems [2]. In both hardware and software domains, there is a great deal of formal and empirical knowledge which guides system architects towards optimal design time decisions, and myriad runtime operation modes (i.e., power saving modes) controlled locally or remotely [3]. Approximate computing promises unprecedented power savings by introducing a trade off between power and another dimension: accuracy [4]. For applications resilient to inaccurate computations [5], or where there isn't a single golden result [6], approximate computing methods can improve traditional design strategies for power reduction: essential in the dark silicon era [7].

Despite its promise, approximate computing is still an immature technology: a formal model of the impact of approximations on other design metrics does not yet exist [8]. Hence, most approximate computing applications require two premises to be implemented successfully: (a) adequate test data are available, to correctly model the accuracy impact

of approximations [9]; and, (b) approximations are performed iteratively at design time, in order to meet the required power/accuracy goals, and remain static throughout deployment [10].

This is a stark contrast to performance/power trade offs, where well established benchmark suites offer near total coverage of application scenarios [11]: in approximate computing, test data that allows adequate modeling of accuracy is often unavailable. In performance/power trade offs, systems can self-tune their operation based on load and run time parameters to dynamically adjust metrics [12]. In approximate computing, approximations are static: mainly because there is no trusted method to determine if accuracy suffices, without access to ground truth [13]. In this paper, we tackle this problem: adjusting the level of approximations at run time, for signal processing applications. Our hypothesis states that prior knowledge about processed data can guide built-in approximation engines, dynamically modifying the level of approximations whilst ensuring that accuracy suffices for the required task.

Specifically, this paper offers the following contributions:

- We introduce the concept of prior knowledge-guided approximations. This represents a statistical measure of approximation impact, unlike test data-based empirical measures prevalent in the state of the art [14].
- We introduce a model of run time approximations, which use prior knowledge to ensure that accuracy suffices, without access to ground truth, unlike iterative comparisons to ground truth prevalent in the state of the art [15].
- We describe and evaluate a proof of concept of our approach, using an Extended Kalman Filter for motion tracking [16], where we have prior knowledge about the target's motion.

The remainder of this paper is organized as follows: Section II describes a top level view of our methodology, explaining how prior knowledge can guide approximations dynamically. Section III describes a case study of our proposed method, where prior knowledge is used to dynamically adjust the approximations applied to an Extended Kalman Filter for tracking. Section IV describes our experimental setup and the obtained results. Finally, Section V presents our conclusions and future work.

## II. LEARNING TO APPROXIMATE

Our methodology is based on equipping the processing pipeline with variable levels of approximation, i.e., configurable approximations, and an approximation engine within a supervisor block (which may contain additional optimisations such as parameter tuning): a block diagram is depicted in Fig. 1. Depending on the application and the deployment technology (e.g., CPU, ASIC, FPGA) the nature of approximations

P. Garcia, M. Emambakhsh and A. Wallace are with the School of Engineering and Physical Sciences, Heriot-Watt University, Edinburgh EH14 4AS, U.K. E-mail: {p.garcia, m.emambakhsh, a.m.wallace}@hw.ac.uk.

Manuscript received XXX XX, XXXX; revised XXX XX, XXXX.

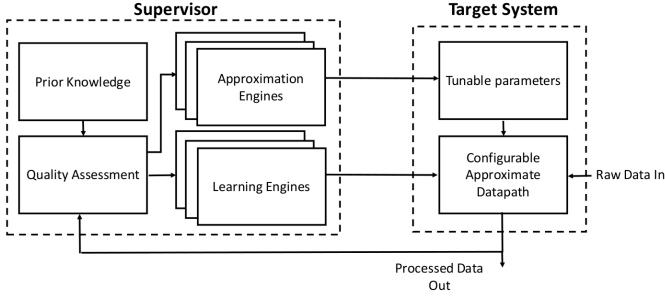


Fig. 1: Block diagram

varies, but our method is applicable across the entire spectrum. Traditional approximation methods include bit width reduction [4], memoisation [17], predictive memory access [18], arithmetic re-writes [10], input-based approximations [19], etc.

Based on prior knowledge about the data, our approximation engine dynamically monitors the processing pipeline's output, and verifies whether or not the calculations still obey the assumptions about the data. If yes, then it is assumed that current levels of accuracy are still within error bounds: hence, the pipeline can be approximated further. If not, then it is assumed that accuracy has exceeded error bounds, and the level of approximation is reduced. This behaviour is described in Fig. 2. Using this method, it is possible to converge on an approximation strategy that optimises power consumption *in situ*, without access to ground truth.

Such comparison with the prior knowledge can be performed in various ways. For an iterative filtering, which estimates and corrects the state of the object using the obtained measurements, the prior knowledge can be defined using the target's motion. Any deviation from this known model can be used to compromise over approximation during run-time.

One solution to quantify such model is to stack state vectors for a given number of consecutive iterations. Then estimating the statistics of the stacked tracks, using either a parametric or non-parametric approaches, can be used to map the result to our prior knowledge.

To be more specific, in this paper, we use a parametric approach to approximate the probability density function (PDF) of the stacked target states from iteration  $k$  to  $k + N$ , i.e.  $s_{k:k+N}$ . Our prior knowledge is then compared with the computed approximated PDF. In our work, we use KullbackLeibler (KL) divergence to perform this task as follows,

$$D_{KL}(\mathbf{H}_{k,N} || \mathbf{H}_p) = \sum_i \mathbf{H}_{k,N} \log \frac{\mathbf{H}_{k,N}}{\mathbf{H}_p} \quad (1)$$

in which  $\mathbf{H}_{k,N}$  is the approximated PDF of the  $k^{th}$  to  $(k + N)^{th}$  state samples and  $\mathbf{H}_p$  is the "prior knowledge" PDF of the target's motion.

Our approach is predicated on runtime-configurable levels of approximation. In software solutions running on CPUs and GPUs, this can be achieved through different software versions [20] or through Instruction Set Architecture (ISA) level approximations [21]. In bespoke hardware solutions implemented on ASIC or FPGA, through configurable hardware

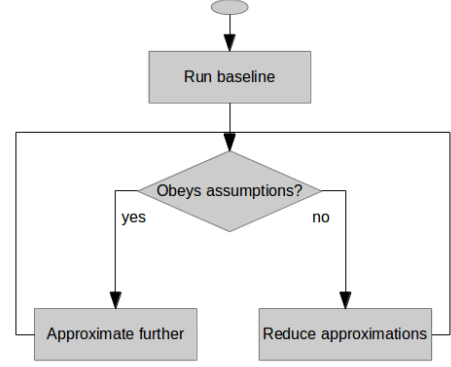


Fig. 2: Approximation engine's runtime behaviour.

versions which clock- or power-gate accurate circuitry [22]; this is the approach we use on our experiments, which we detail in Section IV.

### III. CASE STUDY: EXTENDED KALMAN FILTER TRACKING

The proposed approximate computing algorithm is evaluated for a non-linear, Gaussian, single-target tracking problem. It is assumed that the target is circularly rotating over the  $xy$ -plane. In order to have the paper self-contained as much as possible and to simplify explaining the points at which approximation is imposed, the motion model and EKF equations are detailed in this section.

It is assumed that the sensor measures the range and bearing (azimuth) of the target in meters and radians, respectively, which are as follows,

$$\begin{cases} r_k = \sqrt{\bar{x}_k^2 + \bar{y}_k^2} + n_{r_k} \\ \phi_k = \text{atan2}(\bar{y}_k, \bar{x}_k) + n_{\phi_k} \end{cases}, \quad (2)$$

where  $\bar{x}_k$  and  $\bar{y}_k$  are the true states of the target location,  $\mathbf{Z}_k = [r_k, \phi_k]$  contains the measured range and bearing values, and  $\mathbf{N}_k = [n_{r_k}, n_{\phi_k}]$  is a random vector sampled from a Gaussian with zero mean, and all are at the  $k^{th}$  iteration.  $\text{atan2}(\cdot)$  computes the angle between the point (vector)  $[\bar{x}_k, \bar{y}_k]$  and positive  $x$ -axis.

It is assumed that at time  $k$ , the target has a three dimensional state vector  $\mathbf{X}_k = [x_k, y_k, \theta_k]^T$ , in which  $[x_k, y_k]$  and  $\theta_k$  are the position and pose states of the target, respectively. This is shown in Fig. 3. The state estimation equations are,

$$\begin{cases} \hat{x}_k = x_{k-1} + (\Delta t)v_k \cos(w_k \Delta t + \theta_{k-1}) + m_{x_k} \\ \hat{y}_k = y_{k-1} + (\Delta t)v_k \sin(w_k \Delta t + \theta_{k-1}) + m_{y_k} \\ \hat{\theta}_k = \theta_{k-1} + w_k \Delta t + m_{\theta_k} \end{cases}. \quad (3)$$

$\mathbf{u}_k = [v_k, w_k]$  is the speed vector containing the radial and angular speed parameters in m/sec and rad/sec, respectively, and  $\Delta t$  is the time update resolution in sec.  $\hat{\mathbf{X}}_k = [\hat{x}_k, \hat{y}_k, \hat{\theta}_k]^T$  is the estimated state vector for the  $k^{th}$  iteration.  $\mathbf{M}_k = [m_{x_k}, m_{y_k}, m_{\theta_k}]^T$  is a random vector sampled from a Gaussian distribution with zero mean.

Due to the non-linearity in (2) and (3), Gaussianity will not be preserved and therefore, a linear approximation is used

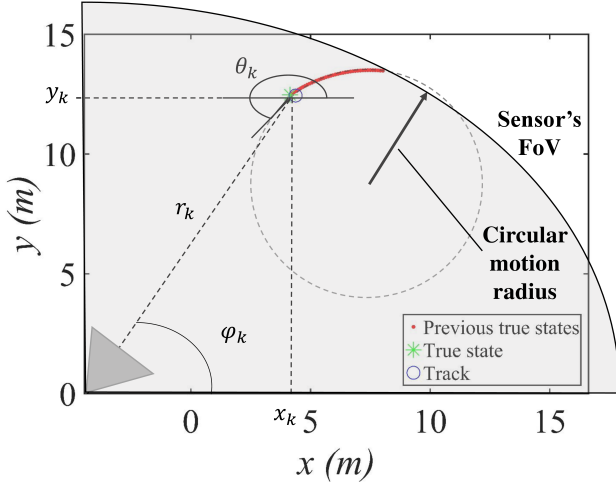


Fig. 3: The tracking scene containing the FoV of the sensor, target motion trajectory and state parameters definition.

based on Taylor series expansion. The Jacobian matrix for the estimation step will be,

$$\mathbf{J}_{X,k-1} = \begin{bmatrix} 1 & 0 & -(\Delta t)v_k \sin(w_k \Delta t + \theta_{k-1}) \\ 0 & 1 & (\Delta t)v_k \cos(w_k \Delta t + \theta_{k-1}) \\ 0 & 0 & 1 \end{bmatrix}. \quad (4)$$

Assuming  $\Sigma_{X,k-1}$  and  $\mathbf{Q}_k$  are the state and noise covariance matrices at  $k-1$  and  $k$ , the estimated state covariance matrix at iteration  $k$  will be:  $\Sigma_{\hat{X},k} = \mathbf{J}_{X,k-1} \Sigma_{X,k-1} \mathbf{J}_{X,k-1}^T + \mathbf{Q}_k$ .

The correction step of EKF incorporates the measurement at time  $k$ . Let  $\mathbf{R}_k$  be the measurement covariance matrix. Then the corrected state vector can be computed as follows,

$$\begin{aligned} \mathbf{X}_k &= \hat{\mathbf{X}}_k + \mathbf{K}_k(\mathbf{Z}_k - h(\hat{\mathbf{X}}_k)) \\ \mathbf{K}_k &= \Sigma_{\hat{X},k} \mathbf{H}_k^T \mathbf{S}_k^{-1} \\ \mathbf{S}_k &= \mathbf{H}_k \Sigma_{\hat{X},k} \mathbf{H}_k^T + \mathbf{R}_k \end{aligned} \quad (5)$$

$\mathbf{K}_k$  is the Kalman gain,  $\mathbf{S}_k$  is the innovation covariance and  $\mathbf{X}_k$  is the (corrected) state vector at the  $k^{th}$  iteration.  $h(\cdot)$  is a non-linear function, which maps the current estimated target state to the coordinate frame of the sensor.  $\mathbf{H}_k$  is the measurement's Jacobian matrix, which is computed as follows,

$$\mathbf{H}_k = \frac{1}{\sqrt{x_k^2 + y_k^2}} \begin{bmatrix} x_k & y_k & 0 \\ -y_k & x_k & 0 \end{bmatrix}. \quad (6)$$

The corrected covariance matrix for the  $k^{th}$  iteration will then be,

$$\Sigma_{X,k} = \left( \begin{bmatrix} 1 & 0 & 0 \\ 0 & 1 & 0 \\ 0 & 0 & 1 \end{bmatrix} - \mathbf{K}_k \mathbf{H}_k \right) \Sigma_{\hat{X},k}. \quad (7)$$

#### A. KL divergence for Gaussian motion

For this experimental setting, we assume that the object's motion statistics remains Gaussian (our prior knowledge). This can be iteratively evaluated by (1). It can be easily shown that the KL divergence for two Gaussian distributions can be simplified as follows,

$$D_{KL}(\mathbf{H}_{k,N} || \mathbf{H}_p) = \log \frac{\sigma_p}{\sigma_{k,N}} + \frac{\sigma_{k,N}^2 + (\mu_{k,N} - \mu_p)^2}{2\sigma_p^2} - \frac{1}{2} \quad (8)$$

in which,  $(\mu_{k,N}, \sigma_{k,N}^2)$  and  $(\mu_p, \sigma_p^2)$  are the mean vector and variance of the stacked states and prior knowledge, respectively. For our experiments, we assume that  $\mu_p$  is the radius of the target's circular rotation, which is known with a  $\pm \sigma_p$  standard deviation (both in meters).

We define the stacked state samples  $\mathbf{s}_{k:k+N}$  as the Euclidean distance between the target state  $[x_k, y_k]^T$  and centre of rotation. Using the stacked samples  $\mathbf{s}_{k:k+N}$ ,  $\mu_{k,N}$  and  $\sigma_{k,N}$  are then computed as follows,

$$\begin{aligned} \mu_{k,N} &= \frac{\sum_i \mathbf{s}_{k:k+N}}{N} \\ \sigma_{k,N}^2 &= \frac{\sum_i (\mathbf{s}_{k:k+N} - \mu_{k,N})^2}{N} \end{aligned} \quad (9)$$

Small values for  $D_{KL}(\cdot)$  correspond to higher similarity between the prior knowledge and tracks. Therefore, more intense approximation is imposed. On the other hand, the approximation level is reduced once the  $D_{KL}(\cdot)$  is higher than a given threshold.

## IV. EXPERIMENTAL RESULTS

Fig. 4 presents our methodology to obtain accuracy and power profiles for several degrees of approximation, and to generate a version with configurable approximations.

We begin by implementing EKF in Matlab in applying several algorithm-specific approximations (described in detail in Sub-Section IV-A). Matlab simulations are performed to obtain accuracy profiles for each approximation at this step. Matlab Coder is then used to generate C code corresponding to the exact and various approximated versions. C code generated by Matlab is not directly synthesizable to FPGA: hence, we refactor it manually to obtain synthesizable versions. Functionality and corresponding accuracy are not affected by this step. We then apply algorithm-independent approximations on this refactored C code, and use a High Level Synthesis tool (Xilinx Vivado HLS) to generate Verilog Hardware Description Language (Verilog HDL) exact and approximated versions. Matlab's HDL coder offers a direct route from Matlab to FPGA, but not all language constructs are supported and it would not enable us to perform algorithm-independent optimisations: hence the use of HLS through Xilinx's tools.

RTL simulation and FPGA synthesis (we target Virtex 7 technology) is performed through Xilinx Vivado Design Suite to obtain resource usage and power consumption. Power consumption is estimated through Xilinx Power Estimator tool embedded in Vivado, which uses resource usage information and switching rates obtained from RTL simulation to calculate a high accuracy measure of power consumption. This step enables us to obtain power profiles for each approximation.

The final step combines the various versions into one configurable solution. This is an FPGA implementation which combines accurate and approximated versions, where the level of approximations can be configured and modified at runtime. Unused logic (e.g., an exact version of some operation when

running in corresponding approximate mode) is clock gated to eliminate dynamic power consumption. This version is then used to obtain results for dynamic approximations by the approximation engine using prior knowledge.

#### A. Power and Accuracy Profiles

Algorithm-dependent approximations are modifications on the implementation of certain constructs, which vary from algorithm to algorithm. These can be complete re-writes of algorithm functionality; however, since our goal is to determine the validity of prior knowledge for runtime approximations, simple arithmetic re-writes suffice. We implemented four different re-writes:

- 1) COS re-write: cosine functions are replaced by quantized look-up tables. The HDL implementation of cosines is realized through a look-up table, but by re-writing at Matlab level, we can control the level of quantization: the approximated version is more quantized (i.e., requires fewer data) than the default Vivado HLS implementation.
- 2) SIN re-write: identically to cosine, sine functions are re-written using a quantized loop-up table.
- 3) SQRT re-write: the square root of the sum of squares  $\sqrt{x^2 + y^2}$ , which requires two DSP multipliers and a look-up table for the square root, is replaced by a sum of absolutes  $|x| + |y|$ , which requires only two conversions to unsigned and an adder.
- 4) ATAN re-write: the arc tangent function, realized by default through a look up table, is approximated through the first three terms of a Taylor series, requiring only arithmetic operations.

We detailed several algorithm-independent approximations in Section II. In our experiments, we implemented bit width reduction, from floating to fixed point. The default bit width is 64 bits (Matlab generates double precision floating point operations). Our approximations replaces 64 bits data with fixed point 27 bits data (15 integer and 12 fractional bits). This is one of the fixed point bit widths recommended for power reductions in the Virtex 7 family.

Version	Power (W)			% of baseline
	Static	Dynamic	Total	
Exact	0.247	0.552	0.799	100%
COS	0.247	0.523	0.770	96.37%
SIN	0.247	0.523	0.770	96.37%
SQRT	0.247	0.534	0.781	97.74%
ATAN	0.247	0.532	0.779	97.49%
27 bits Fixed Point	0.246	0.538	0.785	98.24%

TABLE I: Power profiles for exact and each individual approximation.

We ensured that during our RTL simulations, 100 iterations of the complete function are performed, using the same randomly generated input data for all versions, in order to obtain representative activity that ensures high confidence in the power estimation. Table I depicts power consumption for the exact and each individual approximated version. Static power remains constant across approximations because the

contribution of on-chip memories (BRAMs) dominates, and the number remains constant except for a small reduction when reducing bit widths.

Our next set of experiments started measuring the power consumption of versions that combine bit width reduction with several of the other approximations: results are presented in Table II.

Approximations (using 27FP)	Power (W)	% of baseline
COS	0.756	94.61%
SIN	0.756	94.61%
SQRT	0.767	95.99%
ATAN	0.765	95.74%
COS & SIN	0.741	92.74%
COS & SQRT	0.767	95.99%
COS & ATAN	0.736	92.11%
SIN & SQRT	0.738	92.36%
SIN & ATAN	0.736	92.11%
SQRT & ATAN	0.747	93.49%
COS & SIN & SQRT	0.709	88.73%
COS & SIN & ATAN	0.707	88.48%
COS & SQRT & ATAN	0.718	89.86%
SIN & SQRT & ATAN	0.718	89.86%
COS & SIN & SQRT & ATAN	0.689	86.23%

TABLE II: Power profiles for combinations of different approximations.

We use Matlab simulation to determine the accuracy of each combination, compared to the baseline. Table III depicts the accuracy of each version. Results in the "Absolute" tab are the mean and standard deviation ( $\sigma$ ), respectively, of the absolute error (in meters) compared to the ground truth (real object position) in our simulation. Results in the "Accuracy" tab are the ratios, for mean and standard deviation, between the exact version results and the absolute value of the difference between exact and approximate results.

Version	Absolute (m)		Accuracy (%)	
	Mean	$\sigma$	Mean	$\sigma$
Exact	0.5633	0.3092	100	100
COS	0.6742	0.2805	83.55	89.76
SIN	0.6524	0.3652	86.34	84.66
SQRT	0.6968	0.3764	80.84	82.14
ATAN	3.3520	1.7953	16.80	17.22
COS & SIN	0.6044	0.3973	93.19	77.82
COS & SQRT	0.7497	0.4101	75.13	75.39
COS & ATAN	0.9771	0.6937	57.65	44.57
SIN & SQRT	0.7353	0.3711	76.60	83.31
SIN & ATAN	7.7667	2.5248	7.252	12.24
SQRT & ATAN	1.4812	0.8149	38.02	37.94
COS & SIN & SQRT	0.5870	0.3680	95.96	84.02
COS & SIN & ATAN	1.7503	1.0135	32.18	30.50
COS & SQRT & ATAN	0.9949	0.7006	56.61	44.13
SIN & SQRT & ATAN	7.7528	2.5424	7.265	12.16
COS & SIN & SQRT & ATAN	1.8295	1.0765	30.78	28.72

TABLE III: Accuracy profiles for combinations of different approximations. Exact version uses double floating point precision (64 bits); every other version uses 27 bits fixed point precision.

The final integrated version with configurable approximations, including clock gated logic, is compared against the baseline in Table IV.



	Power (W)			FPGA Resources			
	Static	Dynamic	Total	LUT	FF	DSP	BRAM
Exact	0.247	0.552	0.799	46449	17666	61	55
Approx.	0.246	0.443	0.689	44995	16981	58	55

TABLE IV: Resource usage and power consumption for baseline and final configurable approximations version.

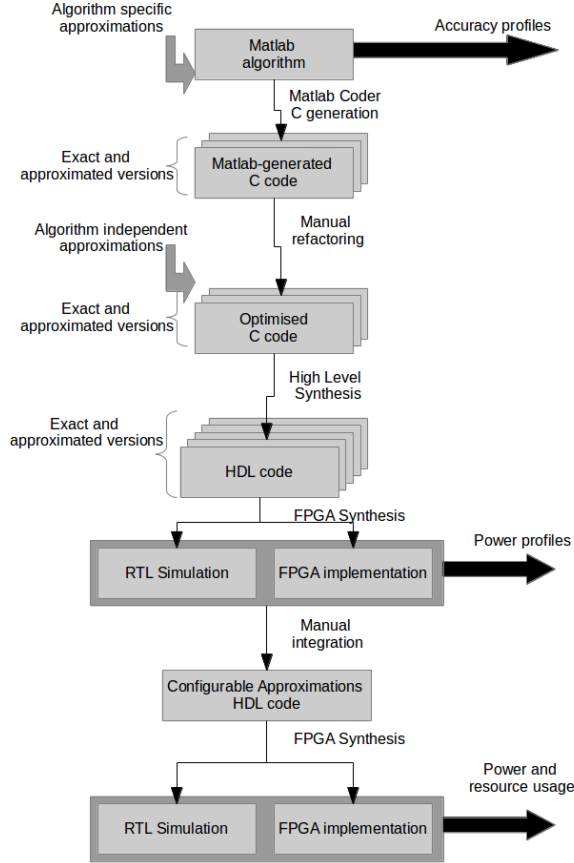


Fig. 4: Experimental design flow.

### B. Dynamic approximations using prior knowledge

The results of dynamically performing the approximation using the algorithms explained in Section II and III are detailed here. First, using the approximation results of each individual step, an "approximation level" is defined. To do this, various combinations of the micro approximations are sorted in ascending order according to their accuracy error. This results in a vector of tuples containing pairs of indexes (used as the approximation level) and strings indicating the approximation combination.

The first tuple in this vector corresponds to the approximation method, which generates the highest accuracy. Its last element, however, creates the weakest accuracy. At each filtering step, in order to use different approximation combinations, the approximation level is either increased or decreased. Determining whether to increment or decrement the approximation level is performed by evaluating the KL divergence result (8).

The result of the overlay tracking plot using dynamic

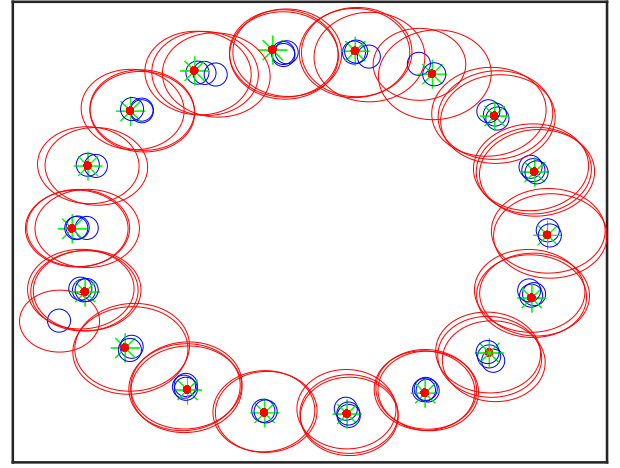


Fig. 5: Every 100 iteration overlay plot of the tracks and true states for an overall 5000 iterations.

approximation in various iterations is shown in Fig. 5 for a total number of iterations 5000. The red ellipses represent the covariance matrix  $\Sigma_{X,k}$  (7) at every iteration, the blue circles show  $[x_k, y_k]^T$  and green asterisks with red dots are the locations of true states  $[\bar{x}_k, \bar{y}_k]^T$ .

At every iteration, KL divergence is computed according to (8), with sample stack size  $N = 75$ . If it is less than a given threshold  $T$  (for our results in Fig. 5,  $T = 0.5$ ) the approximation level is incremented. Otherwise, it is decremented to have a more precision tracking performance. The Euclidean distance between the found track and true state is computed for each iteration and shown in Fig. 6-a, as well as the KL divergence in Fig. 6-b. When the KL divergence goes above  $T$  in Fig. 6, the accuracy deteriorates. The approximation level is then immediately reduced in order to compensate the accuracy. Therefore, in only a few more iterations the accuracy again increases. This causes median accuracy error of 0.1661 (m) with median KL divergence 1.2098 for 5000 iterations.

Using the power profiles in Table II, the consumed energy of each approximation can be computed by multiplying the power with the time resolution ( $\Delta t = 0.1$  (s)). The accumulated energy is plotted in Fig. 7 for the last 1500 iterations. The baseline which consumes a constant power of 0.799 (W), results in a total of  $\approx 394$  (J). However, the accumulated energy consumption for the dynamic approximation case is  $\approx 384$  (J). This shows about 2.54% energy reduction. By compromising over the accuracy result and increasing the KL divergence threshold, more intense approximations can be obtained, which results in even lower energy consumption. This is shown in Fig. 7 as the dashed green and cyan lines for thresholds 1.5 and 4.0, respectively

## V. CONCLUSIONS AND FUTURE WORK

### ACKNOWLEDGMENT

We acknowledge the support of the Engineering and Physical Research Council, grant references EP/K009931/1 (Programmable embedded platforms for remote and compute intensive image processing applications), EP/K014277/1 (MOD

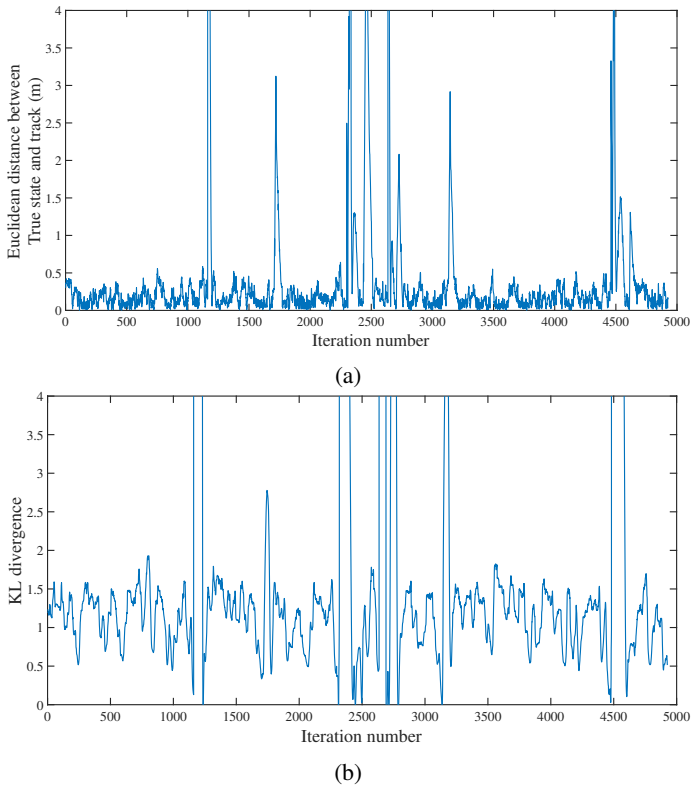


Fig. 6: (a) Euclidean distance between the true state and tracks; (b) Corresponding KL divergence.

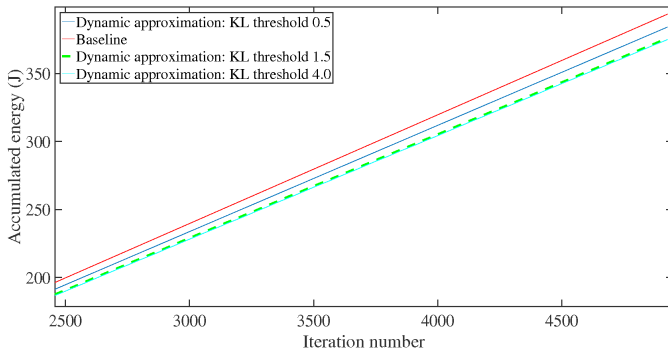


Fig. 7: Accumulated energy consumption for the baseline (no approximation) and dynamic approximations, with three different KL divergence thresholds.

University Defence Research Collaboration in Signal Processing) and EP/N012402/1 (TASCC: Pervasive low-TeraHz and Video Sensing for Car Autonomy and Driver Assistance (PATH CAD)).

## REFERENCES

- [1] V. Vassiliadis, K. Parasyris, C. Chaliros, C. D. Antonopoulos, S. Lalis, N. Bellas, H. Vandierendonck, and D. S. Nikolopoulos, "A programming model and runtime system for significance-aware energy-efficient computing," *SIGPLAN Not.*, vol. 50, no. 8, pp. 275–276, Jan. 2015.
- [2] S. Das, J. R. Doppa, P. P. Pande, and K. Chakrabarty, "Reliability and performance trade-offs for 3d noc-enabled multicore chips," in *Design, Automation & Test in Europe Conference & Exhibition (DATE)*, 2016. IEEE, 2016, pp. 1429–1432.

- [3] S. Senni, L. Torres, G. Sassatelli, and A. Gamatie, "Non-volatile processor based on mram for ultra-low-power iot devices," *ACM Journal on Emerging Technologies in Computing Systems (JETC)*, vol. 13, no. 2, p. 17, 2016.
- [4] S. Mittal, "A survey of techniques for approximate computing," *ACM Computing Surveys (CSUR)*, vol. 48, no. 4, p. 62, 2016.
- [5] Q. Xu, T. Mytkowicz, and N. S. Kim, "Approximate computing: A survey," *IEEE Design & Test*, vol. 33, no. 1, pp. 8–22, 2016.
- [6] S. Venkataramani, K. Roy, and A. Raghunathan, "Approximate computing," in *VLSI Design and 2016 15th International Conference on Embedded Systems (VLSID)*, 2016 29th International Conference on. IEEE, 2016, pp. 3–4.
- [7] T. Mitra, T. S. Muthukaruppan, A. Pathania, M. Pricopi, V. Venkataramani, and S. Vishin, "Power management of asymmetric multi-cores in the dark silicon era," in *The Dark Side of Silicon*. Springer, 2017, pp. 159–189.
- [8] S. Venkataramani, S. T. Chakradhar, K. Roy, and A. Raghunathan, "Approximate computing and the quest for computing efficiency," in *Proceedings of the 52nd Annual Design Automation Conference*. ACM, 2015, p. 120.
- [9] A. Yazdanbakhsh, D. Mahajan, H. Esmailzadeh, and P. Lotfi-Kamran, "Axbench: A multiplatform benchmark suite for approximate computing," *IEEE Design & Test*, vol. 34, no. 2, pp. 60–68, 2017.
- [10] K. Nepal, S. Hashemi, H. Tann, R. I. Bahar, and S. Reda, "Automated high-level generation of low-power approximate computing circuits," *IEEE Transactions on Emerging Topics in Computing*, 2016.
- [11] J. L. Henning, "Spec cpu2000: Measuring cpu performance in the new millennium," *Computer*, vol. 33, no. 7, pp. 28–35, 2000.
- [12] C. Isci and M. Martonosi, "Runtime power monitoring in high-end processors: Methodology and empirical data," in *Proceedings of the 36th annual IEEE/ACM International Symposium on Microarchitecture*. IEEE Computer Society, 2003, p. 93.
- [13] V. K. Chippa, S. T. Chakradhar, K. Roy, and A. Raghunathan, "Analysis and characterization of inherent application resilience for approximate computing," in *Proceedings of the 50th Annual Design Automation Conference*. ACM, 2013, p. 113.
- [14] Q. Zhang, F. Yuan, R. Ye, and Q. Xu, "Approxit: An approximate computing framework for iterative methods," in *Proceedings of the 51st Annual Design Automation Conference*. ACM, 2014, pp. 1–6.
- [15] J. Han and M. Orshansky, "Approximate computing: An emerging paradigm for energy-efficient design," in *Test Symposium (ETS)*, 2013 18th IEEE European. IEEE, 2013, pp. 1–6.
- [16] G. Y. Kulikov and M. V. Kulikova, "The accurate continuous-discrete extended kalman filter for radar tracking," *IEEE Transactions on Signal Processing*, vol. 64, no. 4, pp. 948–958, 2016.
- [17] S. Sinha and W. Zhang, "Low-power fpga design using memoization-based approximate computing," *IEEE Transactions on Very Large Scale Integration (VLSI) Systems*, vol. 24, no. 8, pp. 2665–2678, 2016.
- [18] A. Yazdanbakhsh, B. Thwaites, H. Esmailzadeh, G. Pekhimenko, O. Mutlu, and T. C. Mowry, "Mitigating the memory bottleneck with approximate load value prediction," *IEEE Design & Test*, vol. 33, no. 1, pp. 32–42, 2016.
- [19] A. Raha, H. Jayakumar, and V. Raghunathan, "Input-based dynamic reconfiguration of approximate arithmetic units for video encoding," *IEEE Transactions on Very Large Scale Integration (VLSI) Systems*, vol. 24, no. 3, pp. 846–857, 2016.
- [20] V. Vassiliadis, K. Parasyris, C. Chaliros, C. D. Antonopoulos, S. Lalis, N. Bellas, H. Vandierendonck, and D. S. Nikolopoulos, "A programming model and runtime system for significance-aware energy-efficient computing," in *ACM SIGPLAN Notices*, vol. 50, no. 8. ACM, 2015, pp. 275–276.
- [21] S. Venkataramani, V. K. Chippa, S. T. Chakradhar, K. Roy, and A. Raghunathan, "Quality programmable vector processors for approximate computing," in *Proceedings of the 46th Annual IEEE/ACM International Symposium on Microarchitecture*. ACM, 2013, pp. 1–12.
- [22] W.-T. J. Chan, A. B. Kahng, S. Kang, R. Kumar, and J. Sartori, "Statistical analysis and modeling for error composition in approximate computation circuits," in *Computer Design (ICCD)*, 2013 IEEE 31st International Conference on. IEEE, 2013, pp. 47–53.